This is the peer-reviewed, final accepted version for American Mineralogist, published by the Mineralogical Society of America.
The published version is subject to change. Cite as Authors (Year) Title. American Mineralogist, in press.
DOI: https://doi.org/10.2138/am-2024-9393. http://www.minsocam.org/

REVISION 1

Structural variations along the apatite F-OH join: II. The role of hydrogen bonding in fluoridated teeth

JOHN M. HUGHES[1,5,ξ], DANIEL HARLOV[2,3,4], JOHN F. RAKOVAN[5,6], JAMSHID AHMADI[5], MELANIE J. SIEBER[2,7]

[1]Department of Geology, University of Vermont, Burlington, Vermont, 05405, U.S.A.

[2]Deutches GeoForschungsZentrum GFZ, Telegrafenberg, D-14473 Potsdam, Germany

[3]Faculty of Earth Resources, China University of Geosciences, 430074 Wuhan, China

[4]Department of Geology, University of Johannesburg P.O. Box 524, Auckland Park, 2006 South Africa

[5]Department of Geology & Environmental Earth Sciences, Miami University, Oxford, Ohio, 45056, U.S.A.

[6]New Mexico Bureau of Geology and Mineral Resources, New Mexico Tech, 801 Leroy Place, Socorro, New Mexico, 87801, U.S.A.

[7]University of Potsdam, Institute of Geosciences, Karl-Liebknecht-Strasse 24-25, D-14476 Potsdam

ABSTRACT

Fluoride is one of the most consumed pharmaceuticals in the world, and its facility in preventing dental caries is recognized as one of the top 10 public health achievements of the 20th century. Although hydroxylapatite is often used as an analog of dental enamel, the details of the substitution of F for OH in the apatite anion column are not well known. Using new synthesis techniques, this study extends the structure work on $P6_3/m$ apatites along the middle portion of the F-OH apatite join to compositions near the composition of fluoridated human teeth. The first F substituent in hydroxylapatite, near fluoridated dental enamel compositions, is dramatically underbonded by the surrounding Ca2 atoms (0.72 *vu*) in a hydroxylapatite matrix. However, the hydroxyl hydrogen is able to contribute 0.20 or 0.10 *vu* in hydrogen bonding, depending on whether the substitution creates a reversal site in the anion column; this hydrogen bonding alleviates the bonding requirements of the substituent F. As F concentrations increase along the join, the average hydroxyl contributes increasing amounts of hydrogen bonding to the F column anions; to mitigate the loss of its hydrogen bonding, the hydroxyl oxygen migrates toward the

ξ Email: jmhughes@uvm.edu

adjacent mirror plane that contains the bonded Ca2 atoms, and the triangle of bonded Ca2 ions concomitantly contracts. These two mechanisms increase bonding to the column hydroxyl oxygen from the adjoining Ca2 atoms to balance the loss of hydrogen bonding that stabilizes the substituent F column anion and the increasing concentration of underbonded F.

Introduction

A pharmaceutical can be defined as a compound that is used to prevent, treat, or cure a disease; among the most widely administered pharmaceuticals is fluoride (the ionic form of fluorine), administered in several forms. Indeed, in 2018 73.0% of the U.S. population consumed water from community water systems that contain fluoridated water (United States Centers for Disease Control and Prevention 2021) in order to prevent dental caries. Community water fluoridation is recognized as one of the 10 greatest public health achievements of the 20th century, preventing at least 25% of tooth decay in adults and children (American Public Health Association 2021).

In the administration of pharmaceuticals, it is fundamental to understand how that pharmaceutical compound interacts with the human body. Although there are models that conjecture on how the addition of fluoride to the outermost unit cells of human dental enamel can prevent dental caries, there are no quantitative measurements of the changes in the atomic arrangement or bonding that occur in response to fluoridation; human teeth are not well-crystallized or suitable for the high-precision diffraction studies that are necessary to understand the atomic-level interactions with fluorine as a pharmaceutical.

It is well known that inorganic hydroxylapatite, natural or synthetic $Ca_{10}(PO_4)_6(OH)_2$, is an analog for human dental enamel, although the latter also contains several percent of the carbonate anionic complex (Leventouri et al. 2009). Natural mineral samples of hydroxylapatite are not particularly useful in examining detailed atomic arrangements as they apply to human

teeth. Mineral samples are inherently mixtures of the three anionic end-members of apatite, $Ca_{10}(PO_4)_6(OH,F,Cl)_2$, and pure OH end-member minerals are unknown. Even the putative natural hydroxylapatite end-member from Holly Springs, Georgia, USA, has been shown to contain both F and Cl in the anion column, obviating direct comparisons to human dental apatite (Dykes 1971). For this reason, Hughes et al. (2018) attempted to synthesize apatite samples along the F-OH join, and reported the detailed atomic arrangements of apatites in the mid-solid solution range, with anion compositions between and including $[F_{40}(OH)_{60}]$ and $[F_{67}(OH)_{33}]$. However, the attempts to synthesize less F-rich hydroxylapatite to mimic and elucidate the atomic changes that occur with the addition of F to hydroxylapatite through fluoridation were not successful, thus they reported on the middle range of the fluorapatite-hydroxylapatite solid solution only; synthesis of hydroxylapatite with small amounts of substituent F is difficult, particularly with a yield of crystals suitable for single-crystal diffraction studies.

Since that publication, new methods of synthesizing hydroxylapatite with lower F concentrations, of sufficient size for single crystal study, have been devised, and details of that synthesis are given below. The addition of the atomic arrangement of samples with compositions as low as $\sim[F_{10}(OH)_{90}]$ allows us to conjecture on the incorporation of small amounts of F in hydroxylapatite, and comment on the bonding that occurs with the fluoridation of human teeth.

FLUORIDATION OF HYDROXYLAPATITE IN TEETH

The mechanism(s) by which F^- reduces the incidence of dental caries have been investigated in thousands of studies over the last half-century. Numerous reviews on this topic have been published (e.g. Featherstone 1999; Aoun et al. 2018; Epple et al. 2022; ten Cate and Buzalaf 2019). Although numerous mechanisms have been suggested, a high degree of

consensus exists on the following: 1) Promotion of remineralization (new apatite formation after partial dissolution of original tooth material), 2) formation of fluoridated hydroxylapatite during remineralization, and with less CO_3 than the original tooth apatite, 3) antimicrobial properties, affecting bacteria growth and metabolism, 4) surface armoring by F^- sorption to dental hydroxylapatite inhibiting dissolution, 5) F^- incorporation in pre-eruptive tooth apatite, depending on the amount of F^- ingestion, though it is thought to be negligible in preventing dental caries.

Although there are still many questions to be answered there is sufficient evidence that fluoridated hydroxylapatite, with variable amounts of other substituents (e.g. CO_3), can be created in teeth by engineered exposure to F^- (reviews cited above). This may be through the process of diffusion of sorbed F^- into tooth apatite (only in the surface-most regions of crystallites). It is thought that a more important mechanism of fluoridated hydroxylapatite formation is dissolution (demineralization) of original tooth apatite and reprecipitation (remineralization) of new F^- doped hydroxylapatite. Fluoridated hydroxylapatite has a lower solubility than the non-fluoridated species. It is believed that one mechanism for F^- reduction of dental caries is by decreasing the susceptibility of fluoridated hydroxylapatite in teeth to acid dissolution as a result of its lower solubility compared to non-fluoridated tooth apatite.

EXPERIMENTAL

Synthesis of the four low-F samples

The eight most F-rich samples shown in the accompanying figures (between $[F_{40}(OH)_{60}]$ and $[F_{67}(OH)_{33}]$) were reported in Hughes et al. (2018), and that paper contains the experimental details for the synthesis of those samples as well as the sample with composition $[F_{17}(OH_{83})]$, i.e., the most F-rich of the four low-F samples.

We encountered difficulty in synthesizing low-F crystals using the methods detailed in the previous work, and several years were spent in attempts at synthesizing such samples. Using the synthesis methods outlined below, we were successful in synthesizing samples with compositions as low as ~($F_{0.10}OH_{0.90}$), significantly extending the range of samples from the middle portion of the binary join reported earlier. These new syntheses included samples APS-110, APS-125, APS-126, and APS-127a with F contents lower than the hydroxyl-fluorapatites reported by Hughes et al. (2018).

Synthesis of these four fluoridated hydroxylapatite compositions was undertaken at GeoForschungsZentrum, Potsdam, Germany; the syntheses were accomplished by mixing commercial-grade hydroxylapatite (1 μm particle size) with NaF in gram amounts in order to ensure a low weighing error. This nominally consisted of 9.5 – 10 grams of hydroxylapatite + 0.01 – 0.02 grams of NaF mixed with ethanol in an agate mortar using an agate pestle continuously by hand for about 15 minutes to ensure a homogeneous mixture. The hydroxylapatite-NaF mix was then dried at 105 °C for about an hour. A random sampling of approximately 50 – 55 mg of this mix + 7 mg of H_2O was then added to a tempered (1000 °C), 3 mm diameter, 2-cm long Pt capsule that was arc-welded shut at one end. The H_2O was added first. The mix was then added and subsequently packed in. The Pt capsule was then arc-welded shut and placed in the 105 °C oven for 5 – 10 hours, and then weighed again in order to check for leaks. Any capsule showing weight loss greater than 0.02 mg was discarded.

The four synthesis experiments were run at 1100 °C and 300 MPa in the internally heated gas pressure vessel (IHGPV) for 8 days. An example (APS-126) of the basic reaction between the hydroxylapatite and the NaF in an H_2O-rich environment (assuming total reaction) is as follows:

This is the peer-reviewed, final accepted version for American Mineralogist, published by the Mineralogical Society of America.
The published version is subject to change. Cite as Authors (Year) Title. American Mineralogist, in press.
DOI: https://doi.org/10.2138/am-2024-9393. http://www.minsocam.org/

123 $Ca_{10}(PO_4)_6(OH)_2 + 0.04\ NaF = Ca_{10}(PO_4)_6(OH_{0.98}, F_{0.02})_2 + 0.04\ NaOH$

124 All four synthesis capsules were run together at the same time. In the IHGPV, the
125 temperature was measured with 3 S-type thermocouples and calibrated based on measurements
126 of the melting points of NaCl at 843 °C/200 MPa and 904 °C/500 MPa (Akella et al. 1969). The
127 accuracy is about ± 5 °C at 200 MPa and ± 20 °C at 500 MPa. Maximum thermal gradients along
128 the capsules were ± 10 °C. Pressure measurement was done with a strain gauge and was accurate
129 to ± 7 MPa for experiments up to 500 MPa. During the experiment, pressure was controlled
130 automatically to within ±5 MPa using the hydraulic system of the intensifier and a programmable
131 control unit. The samples were heated isobarically at a rate of 30 °C/min and quenched
132 isobarically with quench rates of 150 to 200 °C/min. After the run, the very shiny and slightly
133 deformed Pt capsules were removed, cleaned, and weighed. Any capsules showing weight loss
134 (> 0.05 mg) were discarded. The capsules were punctured and then dried at 105 °C for several
135 hours, and weighed again to determine fluid loss. The dry and recrystallized hydroxylapatite was
136 removed from the Pt capsule, labeled, and stored.

137 **X-ray structure studies**

138 Data from the eight most F-rich samples presented here are taken directly from Hughes et
139 al. (2018), and details of the X-ray structure studies, including CIF files, are contained or
140 referenced therein. The structure of the sample of composition $[F_{17}(OH_{83})]$ was analyzed in the
141 same laboratory using the same procedures detailed in the 2018 work, and the CIF for that
142 sample is on deposit with the present study.

143 Crystals from the three samples with the lowest F contents were significantly smaller
144 than the other samples, presumably due to the different synthesis conditions. To successfully
145 undertake structure studies of those samples, a Bruker D8 Quest single-crystal X-ray

diffractometer with a D8 three-circle goniometer, Mo microfocus (IμS) Kα radiation, and a PHOTON III C7 area detector was employed. The deposited CIF files contain crystal data and data collection/refinement parameters for the three lowest-F samples.

Bonding of the Apatite Column Anions: OH-F

In the $Ca_{10}(PO_4)_6(OH,F,Cl)_2$ system, the anion column accommodates three monovalent species, (OH), F, and Cl. Hughes et al. (1990) detailed the structural accommodation of all three species in hexagonal ternary apatite and demonstrated that a monoclinic ternary apatite also exists. Hughes et al. (2014) examined the details of the atomic arrangement along the F-Cl binary and the structural accommodation of the two anions of disparate size, and Hughes et al. (2016) elucidated the accommodation of Cl and OH along that binary apatite join and demonstrated that three different arrangements of the column anions exist. Hughes et al. (2018) examined the structure along the central portion of the F-OH apatite binary, a binary of particular interest in biological systems. As noted previously, the present work extends the results of Hughes et al. (2018) toward the hydroxyl end-member, and allows conclusions regarding incorporation of substituent F in biological hydroxylapatite such as occurs during the fluoridation of human teeth.

In compositions along the F-OH apatite join, two species occupy the anion column. Figure 1 illustrates the possible positions of the column occupants, OH and F, at two adjacent intersections of the (00ℓ) mirror planes and [001] anion column. The mirror planes occur at z = ¼ and ¾ within each unit cell of $P6_3/m$ apatite, and at each intersection, one of three possible occupants can exist, each with bonds to the three Ca2 ions disposed in a triangle within the mirror plane. If an F ion occurs in that anion column, it lies coplanar in the mirror plane with the

three Ca2 atoms. If a hydroxyl exists at that mirror plane, it will be displaced approximately 0.34 Å above *or* below the plane due to its slightly larger size (see depiction of OH_{above} and OH_{below} in Fig. 1), bonding to the three Ca2 atoms at slightly longer lengths than the aforementioned Ca-F bonds. In every case, the hydrogen atom of the hydroxyl is directed away from the mirror plane, leading to the possibility of hydrogen bonding within the anion column. Thus, of interest are the steric interactions between OH and F in neighboring sites in the anion column, particularly near the OH end of the F-OH join; that compositional region mimics the composition of fluoridated hydroxylapatite in teeth. Given the reported structures, we can examine the changes that occur with decreasing fluoridation along the fluorapatite-hydroxylapatite join, as well as calculate the strength and direction of the bonding impinging on each column anion. Keep in mind that the conclusions are based on X-ray structure studies that average over the entire crystal.

In pure hydroxylapatite, $[F_0(OH)_{100}]$, the hydroxyl in any individual anion column will be ordered as all OH_{above} *or* OH_{below}, as there are no vacancies or impurities to reverse the anion sequence at any of the column anion sites; this leads to $P2_1/b$ monoclinic apatite (Elliot et al. 1973). However, in geologic apatite, this has not been observed, as sufficient impurities apparently exist to provide reversal sites for the hydroxyls, and there is probably sufficient Type A carbonate substitution in dental enamel to also provide reversal sites. However, the presence of monoclinic zones in hydroxylapatite does not obviate the discussion of hydrogen bonding in this work.

In pure hydroxylapatite, there is weak hydrogen bonding between adjacent hydroxyls that are ordered in the same sense, i.e., both OH_{above} or OH_{below}. For example, in Fig. 1, a hydroxyl disordered below the plane at $z = ¾$ will lead to a neighboring OH_{below} associated with the adjacent mirror plane, at $z = ¼$. The O – O distance will be $c/2$, or ~3.44 Å, which will yield a

hydrogen bond length (O – H ··· O) length of 2.49 Å, using the method of Brown and Altermatt (1985) wherein H ··· O = [(O – O) - 0.95 Å]. That hydrogen bond length yields a hydrogen bond strength of 0.08 *vu* (Ferraris and Ivaldi 1988; all H-bond calculations assume a linear O – H ··· O sequence, in accord with the $P6_3/m$ symmetry). Thus, a hydroxyl oxygen in end-member hydroxylapatite receives 1.92 *vu* in charge-balancing bonding: [(3 x 0.307) = 0.92 *vu*] (Fig. 2) from Ca2, and a net sum of 1.00 *vu* from the two neighboring H atoms (i.e., (1.00 – 0.08) *vu* direct donor – H bonding and 0.08 *vu* in H ··· acceptor hydrogen bonding from the immediately adjacent hydroxyl)]. This bond valence sum of 1.92 *vu* is a nearly ideal value for the hydroxyl oxygen. We note that the situation of the incorporation of the first F substituent is essentially an equivalent model for fluoridated teeth, as fluoridated human dental enamel incorporates only up to about 2000 ppm of fluorine (Robinson et al. 1996). This model demonstrates the method of stabilization of the fluoride substituent in human teeth.

As fluorine is incorporated into the anion column, the bonding incident upon the column anions changes. Consider the first F atom incorporated into hydroxylapatite. Referring to Fig. 1, if that first F ion is incorporated in the mirror plane at $z = ¼$, it will reside in the special position at 0,0,1/4. For F, the bonding environment in a hydroxylapatite matrix is "uncomfortable"; the F substituent receives only 0.72 *vu* of charge balance from the surrounding coplanar Ca triangle and thus is significantly underbonded (Fig. 3). This underbonding is alleviated, however, by the hydrogen bonding contributed by neighboring OH ions. Examining the H ··· F bonding from the H atom associated with the $z = ¾$ hydroxyl, the H ··· F distance, smaller than the H ··· O distance between two OH groups because of the displacement of OH, is now ~2.14 *vu* (Fig. 4), yielding a bond valence of 0.10 *vu* (Brown and Altermatt 1985). The F column anion, underbonded with its

bonds from Ca, thus gains 0.20 *vu* from H ··· F hydrogen bonding, contributed from both sides of the F ion, yielding a comfortable bond-valence sum of 0.92 *vu* (Fig. 4).

It is clear that a local fluorine environment must also exist wherein the ion receives H-bonding from only one side in any individual column. Young et al. (1969), suggested that if the sense of the hydroxyl hydrogen was not reversed, and the F received hydrogen bonding from only one direction, the F would be displaced *ca*. 0.10 Å toward the hydrogen-bonded hydroxyl. Although difficult to observe in diffraction experiments, we did not observe this shift even when the F atom was initially displaced from the special position in the structure modeling. In addition, a 0.10 Å shift of the F ion would yield little additional hydrogen bonding to the F column anion because of the flatness of the hydrogen-bond distance *vs* hydrogen-bond valence in that region (Brown and Altermatt 1985). Thus, that first F column anion incorporated into hydroxylapatite would have an incident bond valence of 0.82 *vu* if H-bonding was received from one side, as opposed to 0.92 *vu* at a reversal site with incident H-bonding from the +/- [001] directions.

Because we know the position of the O(H) atom as a function of F *apfu* (Fig. 5) and the strength of the bonds to F and O(H) from the surrounding Ca2 atoms (Figs. 2, 3), we can extend the curves of Hughes et al. (2018) and comment on the incident bond strength to the F and OH column anions over the portion of the F-OH binary that has been synthesized and studied. The bond-valence sum from the surrounding Ca2 atoms to the individual column anions is displayed graphically in Figure 6. As seen therein, at apatite composition of F_0, essentially equivalent to fluoridated dental enamel (which has an F content of approximately $[F_{0.02}(OH)_{99.98}]$), an F column anion is quite underbonded at 0.72 *vu*, and a hydroxyl oxygen has a bond valence of 0.92 *vu*. The underbonding of the "first F substituent" is modified by 0.20 or 0.10 *vu* of hydrogen

bonding, alleviating the underbonding as discussed earlier and allowing the bonding of F substituents to reach acceptable levels. As additional F substitutes, a larger portion of the donor – H direct hydrogen bonding is shed from the average hydroxyl oxygen in the structure to alleviate the underbonding of the additional F ion. Thus, for the average hydroxyl, the hydroxyl oxygen must contribute more H – Receptor bonding to each substituent F ion, concomitantly reducing the average Donor – H bonding to the hydroxyl oxygen. This reduced bonding from the hydrogen to the hydroxyl oxygen must be balanced by increased bonding from the triangle of Ca2 atoms.

As F-content increases in compositions along the join, the decreased donor-H bonding received by the hydroxyl oxygen is compensated by increased bonding from the Ca2 atoms by two methods. Figure 5 illustrates the shift of the O(H) toward its associated mirror plane, thus decreasing the Ca2 – OH bond distance and concomitantly increasing the bond-valence received by the O(H) column anion from the Ca2 atoms in the (00ℓ) triangle of Ca2 atoms. In addition to this shift of the O(H), Figure 7 illustrates the contraction of the Ca2 triangle, also decreasing the Ca2 – O(H) distance. The combined effect of these two bond-distance diminutions, and concomitant bond-strength increase is illustrated in Figure 2. Figure 6 (middle line) illustrates the remarkable stability in bond valence delivered to the anion column over the range of compositions studies. The summed bond valence impingent on column F and OH, weighted by the relative amounts of each anion, sums between 0.93 and 0.96 *vu* over the entire range of samples, not including the intracolumn bonding of 1.00 *vu* for each hydroxyl.

Implications

The addition of trace amounts of fluoride to human dental enamel has profound effects in preventing dental caries; the process is considered one of the 10 greatest public health accomplishments of the 20th century, and places fluoride among the most consumed pharmaceuticals in the world. However, because of the poorly-crystallized nature of dental enamel and the difficulty in synthesizing crystals along the F-OH apatite join, considered the best analog of human tooth enamel, the environment of low-concentrations of F in a hydroxylapatite matrix is unknown. This work demonstrates that up to ~25% of the bond-valence received by a substituent F column anion is hydrogen bonding; hydrogen bonding is thus essential for stabilization of F in the apatite column of a hydroxylapatite matrix. The series of crystal structures of apatites along the hydroxylapatite-fluorapatite join that are presented in Hughes et al. (2018) and this work allow calculation of bonding environments for column anions along the majority of the F-OH join. The study also illustrates the consistent bond valence delivered to the anion column anionic species over the range of samples studied, as the fluor-hydroxyl atomic arrangement responds to changes in anionic column composition.

Acknowledgments

Support for this work was provided by the National Science Foundation through grants NSF-MRI-1039436 and EAR-1249459 to JMH and EAR-0952298 to JR. The manuscript was improved by reviews by Giovanni Ferraris and an anonymous reviewer; we greatly appreciate the editorial handling by G. Diego Gatta. JMH would also like to acknowledge the late Maryellen Cameron, a mentor, friend, and colleague with whom he began to examine many aspects of apatite crystal chemistry 40 years ago.

References Cited

Aoun, A., Darwiche, F., Al Hayek, S., and Doumit, J. (2018) The Fluoride Debate: The Pros and Cons of Fluoridation. Preventive Nutrition and Food Science, 23(3):171-180.

Akella, J., Vaidya, S.N., and Kennedy, G.C. (1969) Melting of sodium chloride at pressures to 65 kbar. Physical Review, 185, 1135 – 1140.

American Public Health Association (2021) https://www.apha.org/topics-and-issues/fluoridation, accessed October 4, 2021.

Brown, I.D., and Altermatt, D. (1985) Bond-valence parameters obtained from a systematic analysis of the inorganic crystal structure database. Acta Crystallographica, B41, 244-247.

Dykes, E., Elliott, J.C. (1971) The occurrence of chloride ions in the apatite lattice of Holly Springs hydroxyapatite and dental enamel. Calcified Tissue Research, **7,** 241–248.

Elliot, J.C., Mackie, P.E., and Young, R.A. (1973) Monoclinic hydroxyapatite. Science, 180, 1055-1057.

Epple M, Enax J, and Meyer F. (2022) Prevention of Caries and Dental Erosion by Fluorides-A Critical Discussion Based on Physico-Chemical Data and Principles. Dentistry Journal, 10(1):6.

Featherstone, J.D.B. (1999) Prevention and reversal of dental caries: role of low level fluoride. Community Dentistry and Oral Epidemiology; 27:31–40.

304 Ferraris, G. and Ivaldi, G. (1988) Bond valence vs bond length in O ··· O hydrogen bonds. Acta
305 Crystallographica, B44, 341-344.
306 Hughes, J.M., M. Cameron and K.D. Crowley (1989) Structural variations in natural F, OH and
307 Cl apatites. American Mineralogist, 74, 870-876.
308 Hughes, J. M., M. Cameron and K. D. Crowley (1990) Crystal structures of natural ternary
309 apatites: solid solution in the $Ca_5(PO_4)_3X$ (X = F, OH, Cl) system. American
310 Mineralogist, 75, 295-304.
311 Hughes, J.M., Harlov, D., Kelly, S.R., Rakovan, J., and Wilke, M. (2016) Solid solution in the
312 apatite OH-Cl binary system: compositional dependence of solid solution mechanisms in
313 calcium phosphate apatites along the Cl-OH binary. American Mineralogist, 101, 1783-
314 1791.
315 Hughes, J.M., Harlov, D., and Rakovan, J.F. (2018) Structural variations along the apatite F-OH
316 join. American Mineralogist, 103, 1981-1987.
317 Hughes, J.M., Nekvasil, H., Ustunisik, G., Lindsley, D.H., Coraor, A.E., Vaughn, J., Phillips, B.,
318 McCubbin, F.M., and Woerner, W.R. (2014) Solid solution in the fluorapatite -
319 chlorapatite binary system: High-precision crystal structure refinements of synthetic F-Cl
320 apatite. American Mineralogist 99, 369-376.
321 Leventouri, T., Antonakos, A., Kyriacou, A., Venturelli, R., Liarokapis, E., and Perdikatsis, V.
322 (2009) Crystal Structure Studies of Human Dental Apatite as a Function of
323 Age. International Journal of Biomaterials, 2009, 1 – 6.
324 Robinson C, Kirkham J, and Weatherell JA. (1996) Fluoride in teeth and bone. In: Fejerskov O,
325 Ekstrand J, Burt BA, editors. Fluoride in dentistry. Copenhagen: Munksgaard; p. 69–87.

ten Cate, J.M and Buzalaf, M.A.R.. (2019) Fluoride Mode of Action: Once There Was an Observant Dentist . . . Journal of Dental Research, 98(7):725–730.

United States Centers for Disease Control and Prevention. https://www.cdc.gov/fluoridation/statistics/index.htm, accessed October 4, 2021.

Young, R.A., van der Lugt, W., and Elliott, J.C. (1969) Mechanism for fluorine inhibition of diffusion in hydroxyapatite. Nature, 223, 729 – 730.

This is the peer-reviewed, final accepted version for American Mineralogist, published by the Mineralogical Society of America.
The published version is subject to change. Cite as Authors (Year) Title. American Mineralogist, in press.
DOI: https://doi.org/10.2138/am-2024-9393. http://www.minsocam.org/

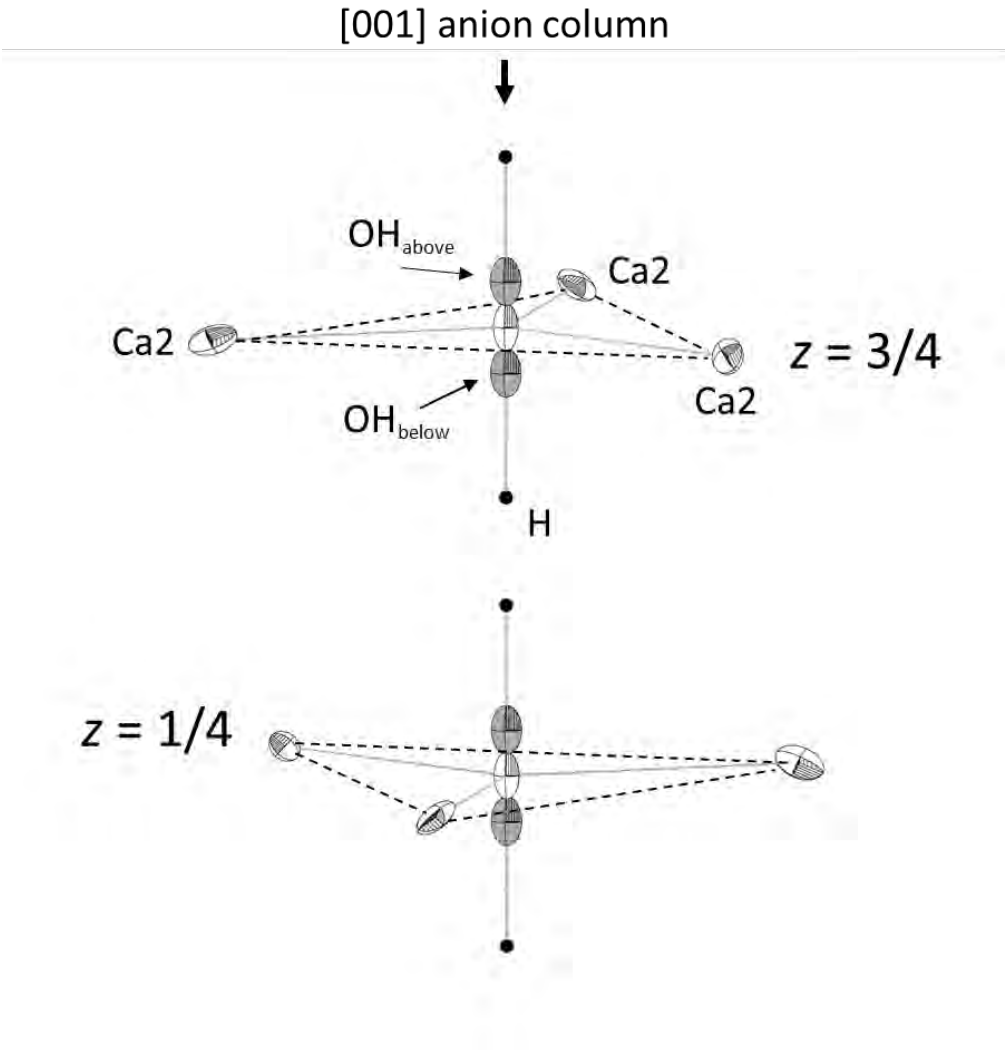

FIGURE 1. Possible positions of OH and F at anion site in anion column of F-OH apatite. The mirror planes (at z = ¼, ¾) in $P6_3/m$ apatite contain the three Ca atoms in the Ca triangle and the F atom in the center of the triangle; Ca - F bonds are shown. The OH (shaded atoms, with bonded black H atoms) positions are ~0.34 Å above or below the mirror plane; the possible Ca2 – OH bonds are not depicted. At any intersection of the anion column and a mirror plane, only *one* of the three depicted anion positions (OH_{above}, F, OH_{below}) is occupied.

This is the peer-reviewed, final accepted version for American Mineralogist, published by the Mineralogical Society of America.
The published version is subject to change. Cite as Authors (Year) Title. American Mineralogist, in press.
DOI: https://doi.org/10.2138/am-2024-9393. http://www.minsocam.org/

345

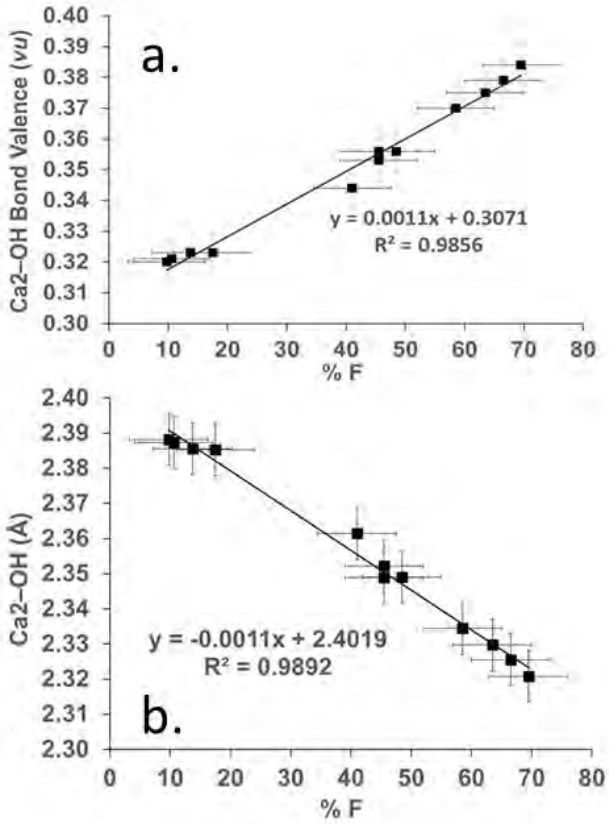

346

347

348

349 **Figure 2**. Relationship between Ca2 – O(H) bond valence (a.) and Ca2 – O(H) bond distance (b.)
350 *vs* % F in anion column. Samples of 40% F and higher were reported in Hughes et al. (2018).

351

352

353

354

355

This is the peer-reviewed, final accepted version for American Mineralogist, published by the Mineralogical Society of America.
The published version is subject to change. Cite as Authors (Year) Title. American Mineralogist, in press.
DOI: https://doi.org/10.2138/am-2024-9393. http://www.minsocam.org/

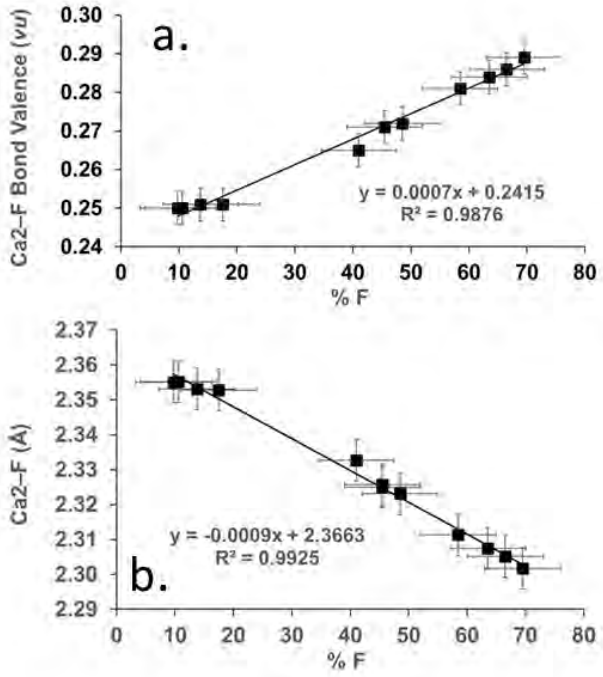

356

357

358

359

360

361 **Figure 3**. Relationship between Ca2 – F bond valence (a.) and Ca2 – F bond distance (b.) *vs* % F
362 in anion column.

363

364

This is the peer-reviewed, final accepted version for American Mineralogist, published by the Mineralogical Society of America.
The published version is subject to change. Cite as Authors (Year) Title. American Mineralogist, in press.
DOI: https://doi.org/10.2138/am-2024-9393. http://www.minsocam.org/

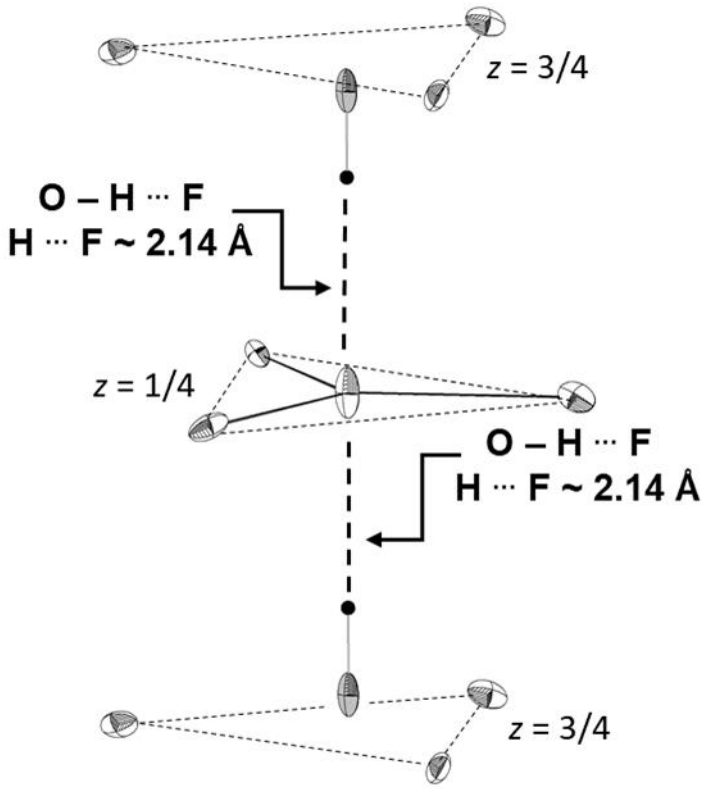

365

366

367 **FIGURE 4**. Depiction of O – H···F hydrogen bonding to F column anion occupant adjacent

368 to two OH occupants disordered toward the F occupant.

369

370

371

This is the peer-reviewed, final accepted version for American Mineralogist, published by the Mineralogical Society of America.
The published version is subject to change. Cite as Authors (Year) Title. American Mineralogist, in press.
DOI: https://doi.org/10.2138/am-2024-9393. http://www.minsocam.org/

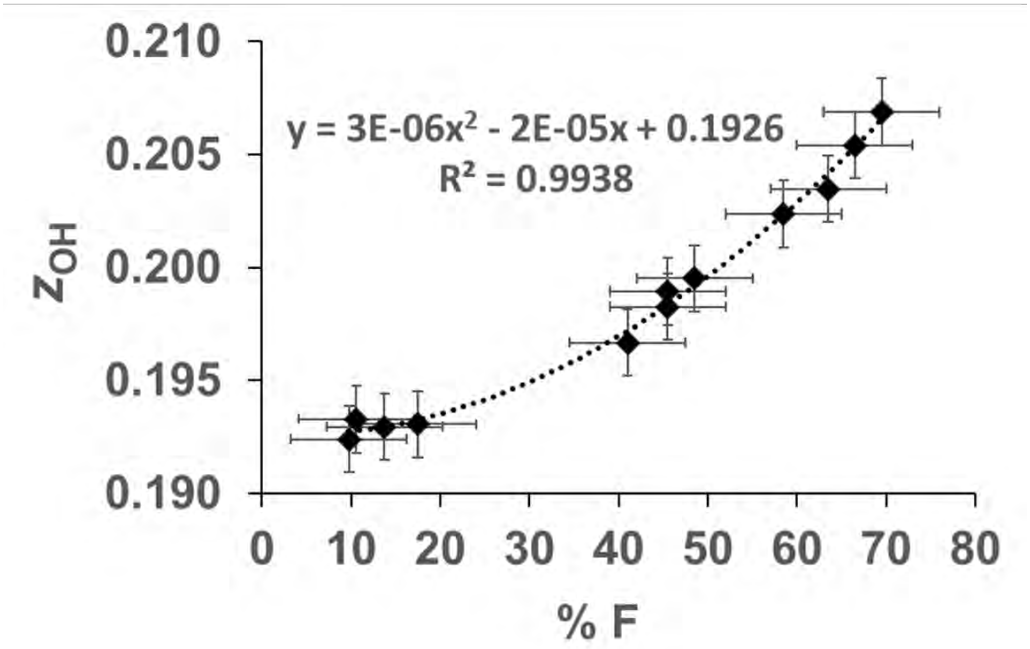

FIGURE 5. Migration of hydroxyl oxygen as a function of % F in anion column.

This is the peer-reviewed, final accepted version for American Mineralogist, published by the Mineralogical Society of America.
The published version is subject to change. Cite as Authors (Year) Title. American Mineralogist, in press.
DOI: https://doi.org/10.2138/am-2024-9393. http://www.minsocam.org/

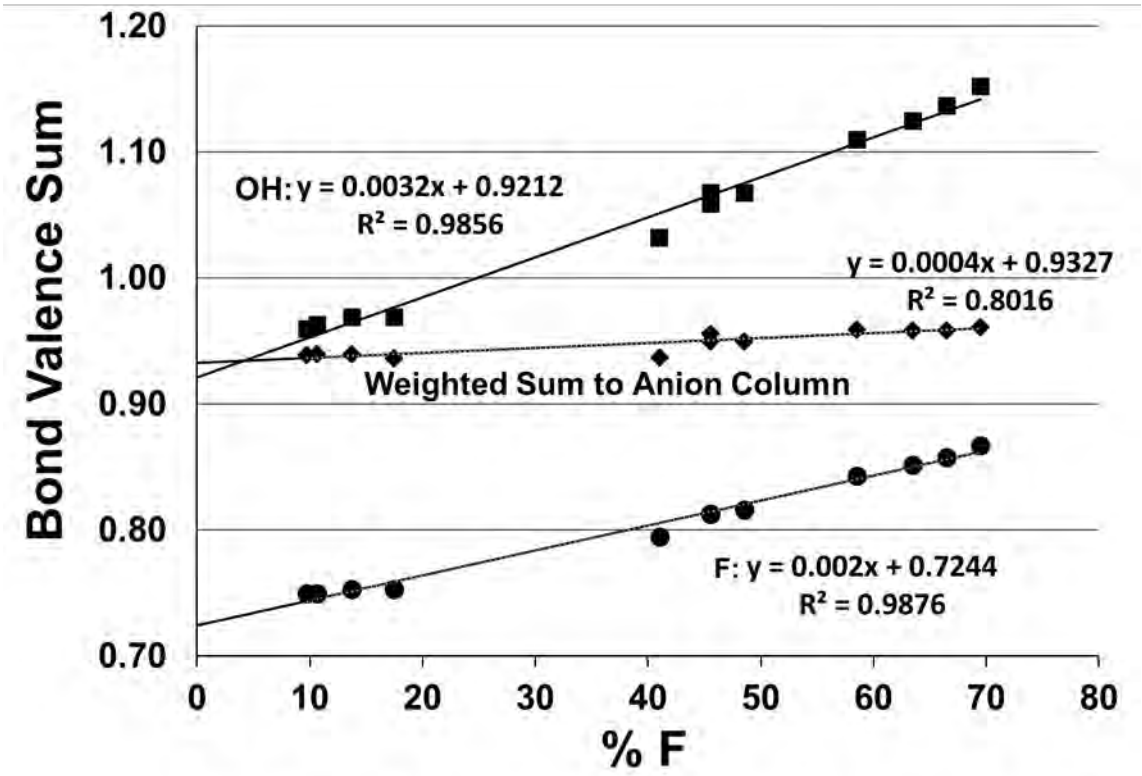

FIGURE 6. Bond valence from Ca2 triangle contributed to hydroxyl oxygen and F ion in apatite anion column for varying F compositions. Upper line is the bond valence contributed to column anion sites occupied by OH, lower line is bond valence contributed to column anion sites occupied by F. The middle line, labeled *Weighted Sum to Anion Column*, is the actual average bond valence contributed to the anion column for study samples as weighted by anion composition.

This is the peer-reviewed, final accepted version for American Mineralogist, published by the Mineralogical Society of America.
The published version is subject to change. Cite as Authors (Year) Title. American Mineralogist, in press.
DOI: https://doi.org/10.2138/am-2024-9393. http://www.minsocam.org/

403

404

405

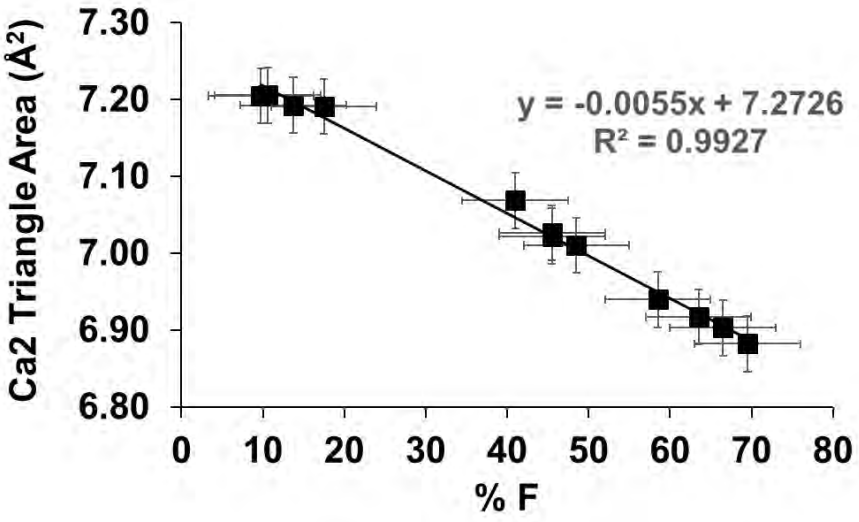

406

407

408 **Figure 7**. Area of (00ℓ) triangles of Ca2 atoms *vs* F content.

409

410

411

This is the peer-reviewed, final accepted version for American Mineralogist, published by the Mineralogical Society of America.
The published version is subject to change. Cite as Authors (Year) Title. American Mineralogist, in press.
DOI: https://doi.org/10.2138/am-2024-9393. http://www.minsocam.org/

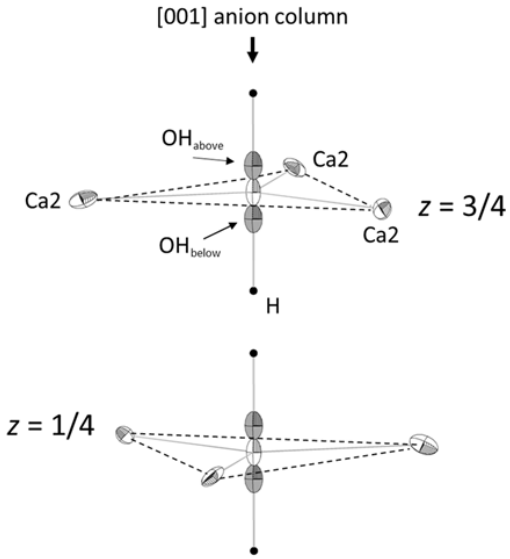

Figure 1.

This is the peer-reviewed, final accepted version for American Mineralogist, published by the Mineralogical Society of America.
The published version is subject to change. Cite as Authors (Year) Title. American Mineralogist, in press.
DOI: https://doi.org/10.2138/am-2024-9393. http://www.minsocam.org/

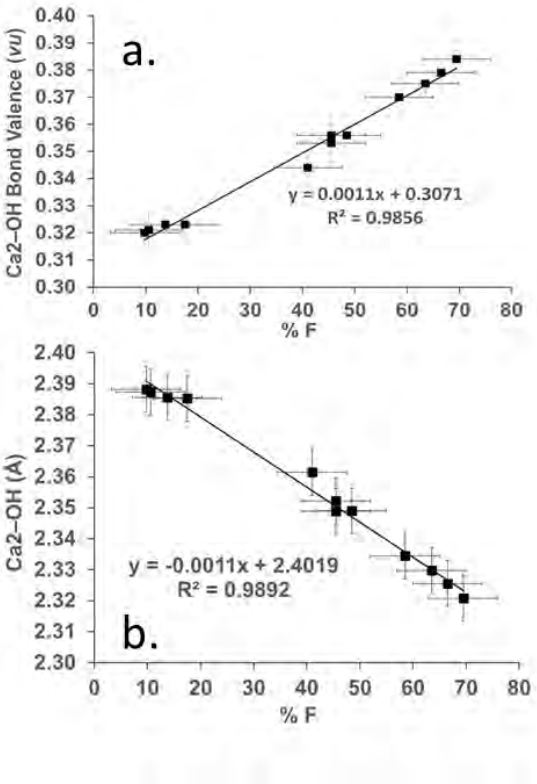

Fig2R1.

This is the peer-reviewed, final accepted version for American Mineralogist, published by the Mineralogical Society of America.
The published version is subject to change. Cite as Authors (Year) Title. American Mineralogist, in press.
DOI: https://doi.org/10.2138/am-2024-9393. http://www.minsocam.org/

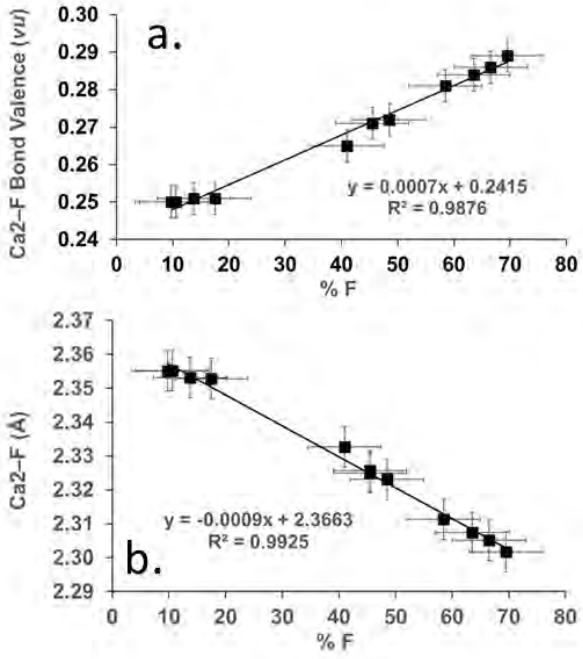

Fig. 3R1.

This is the peer-reviewed, final accepted version for American Mineralogist, published by the Mineralogical Society of America.
The published version is subject to change. Cite as Authors (Year) Title. American Mineralogist, in press.
DOI: https://doi.org/10.2138/am-2024-9393. http://www.minsocam.org/

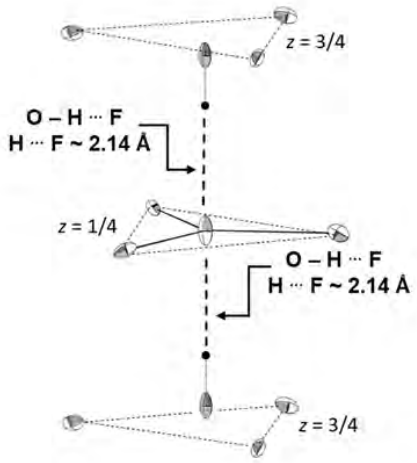

Fig. 4.

This is the peer-reviewed, final accepted version for American Mineralogist, published by the Mineralogical Society of America.
The published version is subject to change. Cite as Authors (Year) Title. American Mineralogist, in press.
DOI: https://doi.org/10.2138/am-2024-9393. http://www.minsocam.org/

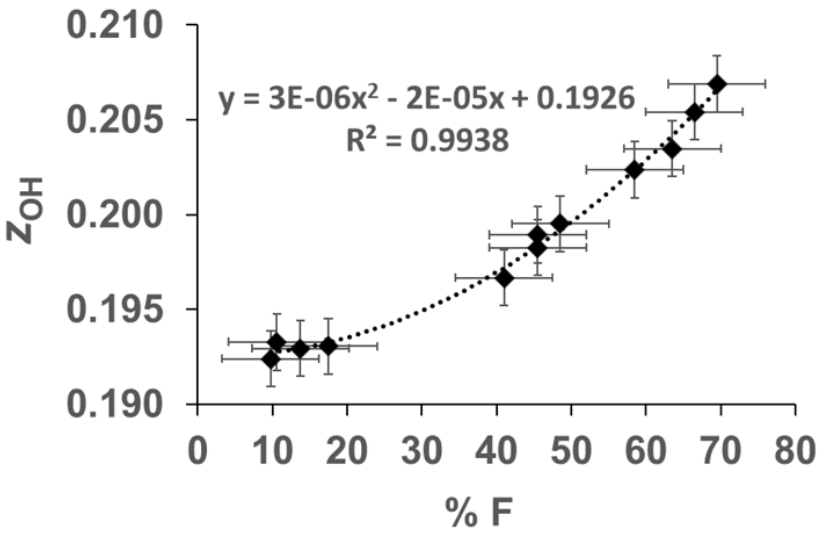

Fig. 5

This is the peer-reviewed, final accepted version for American Mineralogist, published by the Mineralogical Society of America.
The published version is subject to change. Cite as Authors (Year) Title. American Mineralogist, in press.
DOI: https://doi.org/10.2138/am-2024-9393. http://www.minsocam.org/

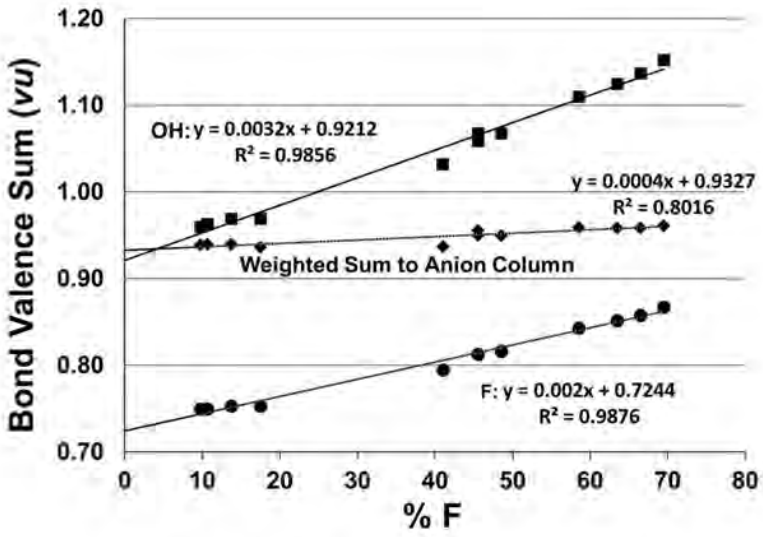

Fig. 6

This is the peer-reviewed, final accepted version for American Mineralogist, published by the Mineralogical Society of America.
The published version is subject to change. Cite as Authors (Year) Title. American Mineralogist, in press.
DOI: https://doi.org/10.2138/am-2024-9393. http://www.minsocam.org/

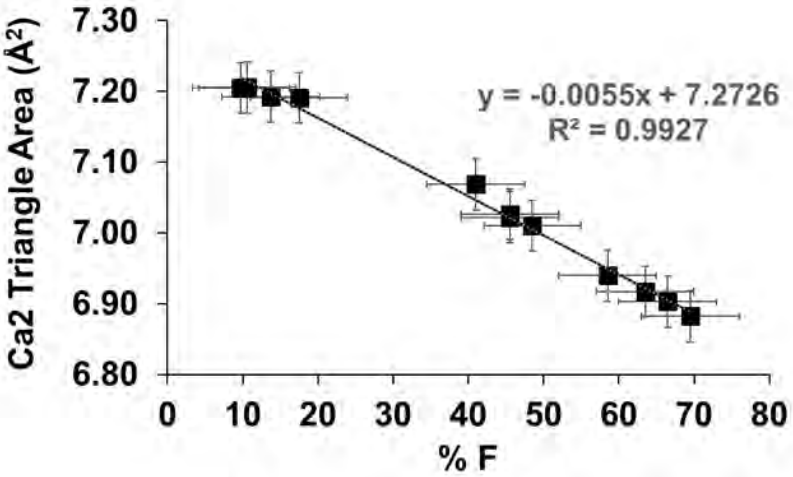

Fig. 7.